Regular article

Friederike M. Möller, Phil Holzmeister, Tapasi Sen, Guillermo P. Acuna* and Philip Tinnefeld*

Angular modulation of single-molecule fluorescence by gold nanoparticles on DNA origami templates

Abstract: We study the angular fluorescence intensity modulation of a single dye positioned near a spherical gold nanoparticle, induced by rotation of linearly polarized excitation light. Accurate positioning and alignment of nanoparticle and fluorophore with respect to each other and the incoming electric field is achieved by a three-dimensional, self-assembled DNA origami. An intensity map is obtained for a fixed distance and two different nanoparticle diameters, revealing polarization-dependent enhancement and quenching of fluorescence intensity in good agreement to numerical simulations.

Keywords: DNA self-assembly; fluorescence modulation; nanoparticles; nanophotonics; single-molecule studies.

*Corresponding authors: Guillermo P. Acuna and Philip Tinnefeld,
NanoBioSciences Group, Institute for Physical and Theoretical Chemistry, TU Braunschweig, Hans-Sommer-Str. 10, 38106 Braunschweig, Germany,
e-mail: g.acuna@tu-bs.de; p.tinnefeld@tu-bs.de
Friederike M. Möller, Phil Holzmeister and Tapasi Sen:
NanoBioSciences Group, Institute for Physical and Theoretical Chemistry, TU Braunschweig, Hans-Sommer-Str. 10, 38106 Braunschweig, Germany

1 Introduction

The interaction between plasmonic nanostructures and fluorescent dyes has been studied extensively both theoretically and experimentally. Even for the basic system of a single metallic nanoparticle and one fluorescent dye, the detailed description is sophisticated and involves many parameters. Within the last years a considerable number of publications focused on specific issues of this interaction such as the dependencies on distance, material, orientation and spectral properties [1–6].

It requires some experimental effort to simultaneously control the fluorophore-nanoparticle distance, the orientation of the connecting axis to the incoming electric field of the excitation beam and the stoichiometry of the nanoparticles with respect to the number of fluorescent dyes. To achieve a detailed experimental picture of the dye-nanoparticle interaction it is essential to extract quantitative information, for which it is advantageous to have a single dye per nanoparticle. Even if the number of dyes is well characterized, heterogeneity of the signal remains because the fluorescence of a single dye also depends on the relative orientation of the dye-nanoparticle axis to the electrical field of the exciting laser beam (and also on the orientation of the dye transition dipole). Again, an averaged view is obtained if the orientation of the dye-nanoparticle axis is not controlled.

Single dye studies were previously performed in a combined fluorescence and atomic force microscopy setup in which a nanoparticle was attached to the tip of the cantilever and a surface with immobilized dyes was scanned [7–9]. Further experimental approaches exploited the rigidity of double stranded DNA which, when used as a spacer, provides a fairly good distance control between dyes and nanoparticle surface. This enabled to obtain a 1:1 stoichiometry for nanoparticle diameters up to 40 nm by electrophoretic separation [10–12].

We and others recently presented a way to increase the size of nanoparticles in nanoparticle-dye constructs while maintaining 1:1 stoichiometry by hybridizing them to surface immobilized dye-labeled DNA origami nanostructures [6, 13]. This is an essential extension because only for gold nanoparticles with a diameter larger than 40 nm the enhanced excitation and radiative rates prevail over the increased non-radiative rate and an overall fluorescence intensity enhancement is observed [7, 14].

In this contribution, we exploit the ability of the DNA origami structure presented in [14], to align the nanoparticle-dye axis with respect to the surface and the incident light to study the angular emission pattern of a single fluorophore near single plasmonic nanoparticles upon rotation of linearly polarized excitation light. The obtained angular fluorescence modulation, not only allows to determine

the orientation of the nanostructure on the surface and hence to maximize the fluorescence, but also to reveal the presence of a nanoparticle without the need for lifetime determination. Furthermore, the system directly visualizes the decoupling of the excitation and emission processes. In this way quantitative information for the nanoparticle induced quantum yield change can be extracted.

2 Materials and methods

We used a self-assembled DNA origami structure [15–17] as a breadboard for the positioning of the single gold nanoparticle (SAuNP) [6, 18] and the single Cy5 dye [14] with nanometer precision. A sketch of the pillar-shaped DNA origami is included in Figure 1A. It has been shown recently that this DNA nanopillar is very stiff and can be placed with a preferential upright orientation on a cover-slip by immobilization with biotin-neutravidin bonds [19]. The DNA origami has a length of 220 nm and a ~14 nm
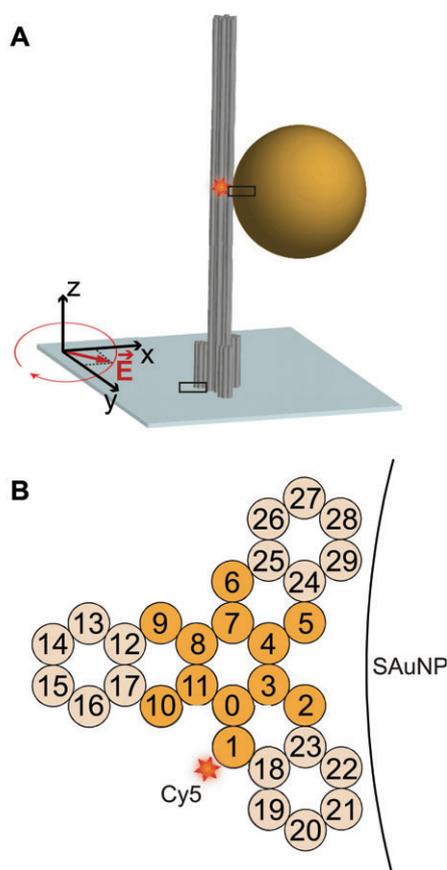

Figure 1 (A) Sketch of the incident E-field polarization and the DNA origami with the SAuNP and fluorescent dye at the equator plane. (B) The numbered helices represent the main structure (0–11) and the base (12–29) in this topview.

diameter consisting of a 12-helix bundle. Three extra 6-helix bundles on the base lead to a base diameter of ~25 nm (Figure 1B, see ref. [14, 19 and 20] for details of the DNA origami design).

We first ensured that the fluorescent dye is free to rotate on the DNA linker faster than the time scale of the measurement so that the dye dipole orientation is averaged. We then attached SAuNPs of 40 and 80 nm diameter at an equatorial distance of ~12.2 nm to the dye and studied the dye-nanoparticle interaction by single-molecule fluorescence lifetime imaging (see the supplementary material for further details). By rotating the excitation laser polarization, the orientation of the 2D projection of the dye-nanoparticle axis is obtained and a map of the dye-nanoparticle interaction is directly measured for a fixed distance.

3 Results

Figure 2A shows fluorescence transients for a DNA origami pillar with an 80 nm, a 40 nm and no SAuNP bound. All transients show the characteristic single bleaching step of single-molecule measurements. Although the excitation polarization is rotated at 5 Hz, the transients reveal no angular dependence if no SAuNP is bound (blue transient), as the Cy5 dye labeled to the 3′ terminus of DNA is able to freely rotate in the sub-microsecond range. Therefore, the dye is excited at all excitation polarizations with equal probability. In contrast, when SAuNPs are added the transients show clear polarization dependence (black and red transients). As the DNA origami structure prohibits direct contact between the SAuNP and the dye in a way that the rotational mobility of the dye is not restricted, we ascribe the modulation to the excitation polarization dependent E-field at the position of the dye. The polar plot in Figure 2B graphically emphasizes the anisotropy and reveals the typical dipole pattern, directly indicating the orientation of the dye-nanoparticle axis.

Concomitantly to the intensity, we followed the fluorescence lifetime of the dyes as shown in the lower panel of Figure 2A. Due to the interaction with the SAuNP, both the radiative and non-radiative rates are enhanced leading to a reduction of the fluorescence lifetime from 1.57 ns to 0.52 ns for the 40 nm SAuNP and 0.41 ns for the 80 nm SAuNP (see Figure 2C for fluorescence decays). The lifetime shortening is a typical indication of the presence of a nanoparticle. By definition, the fluorescence lifetime is the inverse of all rates depopulating the excited state S_1, and therefore characteristic of the emission process.
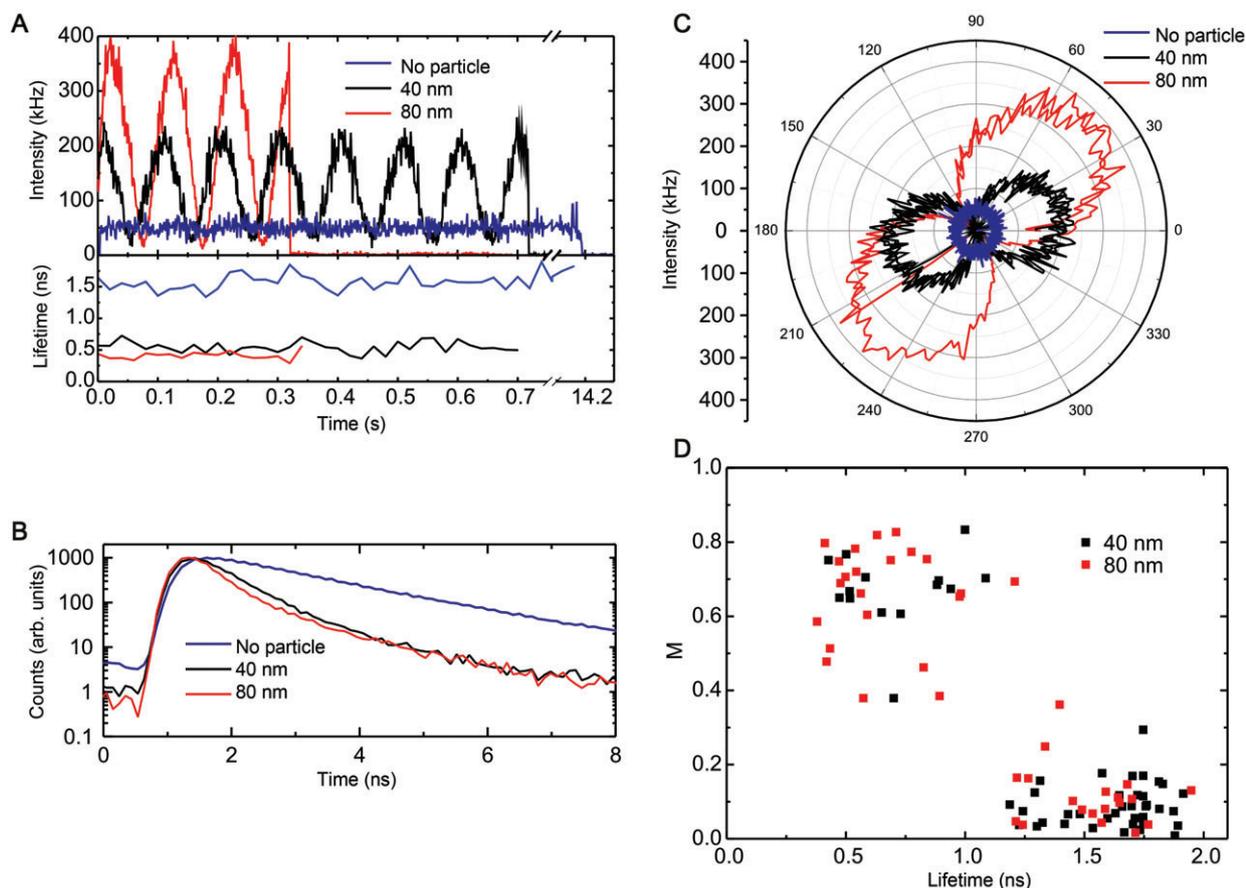
Figure 2 (A) Upper panel, fluorescence intensity transients for the DNA origami structures with no nanoparticle (blue), 40 nm (black) and 80 nm (red) at 1 ms binning. During the measurement, the incident polarization was rotated at a frequency of 5 Hz. Lower panel, corresponding fluorescence lifetime time transient and (B) fluorescence decays. (C) Polar plot showing a dipole-like pattern for the transients with nanoparticle and (D) scatter plot of modulation depth vs. fluorescence lifetime.

The absence of modulation in the lifetime transients upon rotation of the excitation polarization provides direct evidence that for dyes near metals the excitation and emission processes are decoupled.

To quantify the modulation we used the modulation depth M which is a measure of the anisotropy and is defined as $M=(I_{max}-I_{min})/(I_{max}+I_{min})$ [21]. In order to isolate the effect of the polarization rotation on the modulation intensity from different sources of noise, the modulation depth was calculated as $M=I(10\ Hz)/I(0\ Hz)$, where $I(0\ Hz)$ and $I(10\ Hz)$ are the amplitudes of the frequency components at 0 and 10 Hz, respectively, which were obtained using the fast Fourier transform (FFT) algorithm. It has to be noted that because our system is pi-periodic the component at 10 Hz is the relevant one, although the polarization is rotated at 5 Hz. According to the definition, the modulation depth of an isotropic system is close to zero, while highly anisotropic systems exhibit modulation depths near 1. As expected, the dye without SAuNP depicted in Figure 2A yields a low M of 0.04, while the transients

with 40 nm and 80 nm SAuNPs yield M=0.67 and M=0.80, respectively. The distribution of the modulation depth with respect to the fluorescence lifetime is presented in Figure 2D. Two populations can be clearly distinguished. The population with fluorescence lifetime higher than 1.2 ns represents the reference without SAuNP, while the low-lifetime population corresponds to DNA origami pillars with a bound SAuNP. The simultaneous occurrence of fluorescence modulation at rotating excitation polarization (high M) and a decrease of the fluorescence lifetime is a clear signature of nanoparticle binding to the DNA origami. The average M values for the SAuNP population are in a similar range for both nanoparticle sizes because the modulation amplitude and the mean intensity depend on the nanoparticle size, as apparent in the transients.

In the following, we take a closer look at the excitation polarization dependence of the fluorescence intensity for exemplary traces. Generally, the fluorescence intensity of the dye is affected by the nanoparticle's size, shape, distance as well as the orientation of the pillar on the cover

slip surface [19], as the latter determines the alignment of the SAuNP-dye axis relative to the incident electric field. To justify the assumption of a nearly perpendicularly oriented pillar, the transients with the highest count rates out of 21 and 39 fluorescence transients for 40 nm and 80 nm SAuNPs, respectively, are discussed. When the excitation E-field is parallel to the dye-nanoparticle axis, a maximum fluorescence intensity enhancement of approximately 8-fold and 5-fold is obtained for the 80 and 40 nm SAuNP, using the transient without nanoparticle as a reference (Figure 2A).

Interestingly, the transients with bound nanoparticles show modulation minima which exhibit a lower intensity than the average intensity of the dye without nanoparticle. In the minima, the intensity is reduced by a factor of 0.35 for the 80 nm and 0.55 for the 40 nm SAuNP, which translates into overall intensity modulations of 23-fold and 7-fold, respectively. This behavior points towards potential applications in the field of optical switching.

4 Discussion

To quantitatively understand the results, we performed numerical simulations of the electric field intensity (electric field absolute-square) enhancement close to a SAuNP using the commercial FDTD software CST MicrowaveStudio (CST AG). Upon illumination, SAuNPs get polarized. For a SAuNP with dimensions much smaller than the incident wavelength its polarization can be approximated by an electric dipole. In this case the resulting electric field outside the SAuNP is given by the sum of the incident electric field and the dipole-like contribution of the polarized SAuNP. This leads to a particular three-dimensional electric field distribution determined mostly by the polarization of the incident light. Figure 3A and B show numerical simulations of the electric field intensity around SAuNPs with a diameter of 80 and 40 nm, respectively.

At the equatorial plane and close to the SAuNP surface, the interference between both electric field contributions can be constructive or destructive for a fixed distance to the SAuNP but different angles to the incident excitation polarization. In Figure 3C the simulated electric field intensity enhancement is plotted along an orbit at the equatorial plane, 12.2 nm away from the surface of an 80 and 40 nm SAuNP (with phase adapted to the respective transients). As expected, bigger nanoparticles lead to a stronger enhancement of the electric field intensity particularly when oriented along the incident electric field orientation. However, they also lead to a stronger reduction of the electric field at perpendicular orientation. This is due to the fact that in
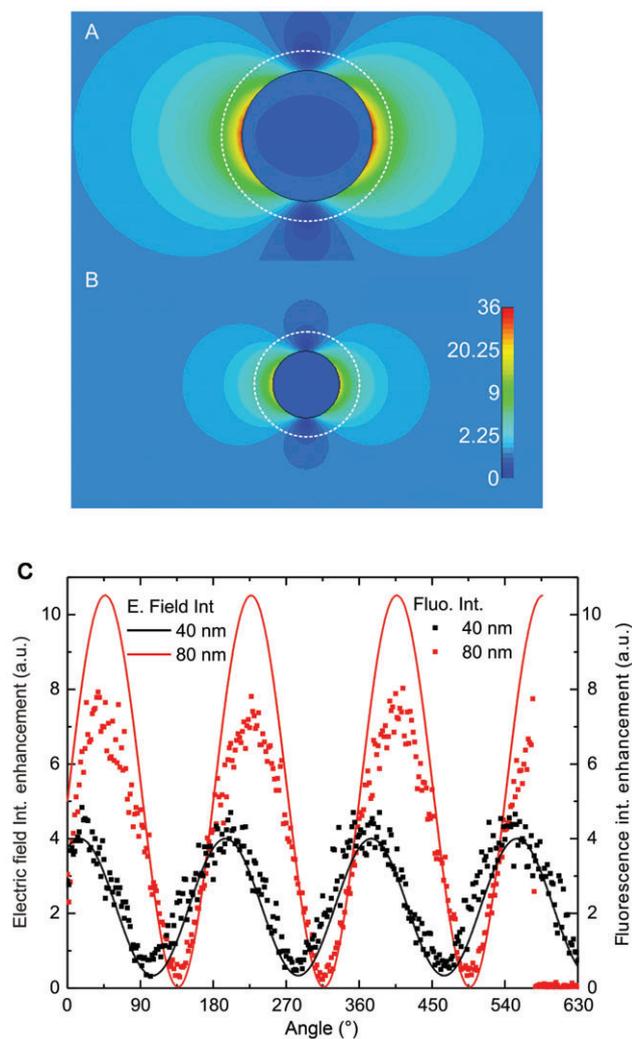

Figure 3 Electric field intensity (electric field absolute-square) at the equatorial plane of an 80 nm (A) and a 40 nm (B) spherical gold nanoparticle. The dotted lines represent the position of the dye at a distance of 12.2 nm to the SAuNP surface. (C) Electric field intensity enhancement along the dotted lines and fluorescence intensity measurements from Figure 2A normalized by the reference transient (fluorescence intensity enhancement). The phase of the simulated field intensity enhancement was adjusted to overlay measurements and simulations.

bigger nanoparticles a greater electric dipole is induced that can partially cancel out the incident electric field at certain positions. This finding is in good agreement with our measurements in which not only an enhancement of the fluorescence intensity was measured but also a reduction for certain excitation polarization angles.

Although the fluorescence intensity modulation included in Figure 2A is related to the relative change in the excitation rate due to the electric field induced by the SAuNP, the presence of the SAuNP also affects the emission properties but independent of the incident electric

field polarization. Thus, by comparing the numerical simulations with our measurements, the relative change in the fluorophore quantum yield induced by the SAuNP can be estimated. In Figure 3C, the fluorescence intensity of the systems with 40 nm and 80 nm SAuNPs normalized to the reference transient without nanoparticle is plotted. The fluorescence intensity enhancement is proportional to the electric field intensity enhancement with the relative change of the quantum yield as the proportionality factor [7, 8]. Changes in the emission pattern of the dye leading to a change of the collection efficiency can be neglected due to the symmetry of our arrangement. A relative change in quantum yield of 1.13±0.31 and 0.72±0.21 was obtained for the 40 and 80 nm SAuNP, respectively. The error takes into account the influence of the measured nanoparticle size distribution on the simulation but other effects, like the deviation in shape and the uncertainty whether binding indeed occurs to all three capturing strands are neglected [6]. Additionally, the numerical simulations assume a planar incidence of the electric field whereas in our experiments, a 1.35NA objective was employed. The relative change in quantum yield q_y' also depends on the orientation of the dye's dipole moment to the SAuNP. Based on ref. [4], q_y' was simulated using the aforementioned FDTD software. For a radial (tangential) orientation q_y' was calculated to be 0.78±0.05 (0.35±0.05) and 1.05±0.05 (0.12±0.04) for 40 and 80 nm, respectively. Generally, it is justified to assume free rotation of the fluorescent dye on the DNA. However, since the time scale of the rotational correlation time (hundreds of picoseconds) is of similar magnitude as the changes of the radiative and non-radiative rates a geometrical averaging cannot be applied. Furthermore, the emission coupling between the SAuNP and the fluorophore is more pronounced for the radial orientation leading to not only a higher quantum yield, but also a lower lifetime. The results are in better agreement with a radial orientation of the dye. This can be explained by the fact that due to the stronger coupling to the SAuNP in the radial orientation, the reduced lifetime biased the decay probability towards radially oriented dyes [14].

A detailed understanding of the interaction of fluorescent dyes with metal nanoparticles requires a precise control not only of the dye-nanoparticle distance and the stoichiometry but also of the orientation of the dye-nanoparticle axis with respect to the polarization of the excitation laser. Here, we used a DNA nanopillar that aligns the nanoparticle-dye axis with respect to the incoming laser illumination. With rotating excitation polarization, pronounced fluorescence modulation is observed in the presence of 40 nm and 80 nm gold nanoparticles next to Cy5 dyes that is accompanied by a shortened fluorescence lifetime. Based on these results, new applications in the field of optical switching can be envisioned. In contrast to previous measurements by Ming et al. [22], ensemble averaging is not required, since 1:1 stoichiometry is achieved in the presented system. Furthermore, the fluorescence modulation does not arise from the intrinsic asymmetric shape of the metallic nanostructure, but is only introduced by the combined system of a quantum emitter and an isotropic nanoparticle. This provides the possibility to detect binding of nanoparticles near emitters without lifetime determination and to identify the orientation of the emitter-nanoparticle system. Moreover, since the signal of a single molecule is measured, the intensity modulations directly 'map' the enhancement field around a SAuNP for a fixed distance of ~12 nm. The performed simulations of the electric field distribution around the nanoparticle further explain more subtle observations such as the drop in fluorescence at excitation polarization perpendicular to the dye-nanoparticle and enable an experimental estimation of the change the fluorescence quantum yield next to the nanoparticle, which is a first step towards an experimental verification of theoretical predictions regarding plasmonic nanoantennas.

The detailed control of the interaction of dyes with metallic nanostructures upon illumination, facilitated by the DNA origami technique has great potential to yield fundamental insights as well as for applications in the field of switching, nanoscale light control and for biomolecular sensing.

References

[1] Coronado EA, Encina ER, Stefani FD. Optical properties of metallic nanoparticles: manipulating light, heat and forces at the nanoscale. Nanoscale 2011;3:4042–59.

[2] Novotny L, van Hulst N, Antennas for light. Nat Photon 2011;5:83–90.

[3] Bek A, Jansen R, Ringler M, Mayilo S, Klar TA, Feldmann J. Fluorescence enhancement in hot spots of AFM-designed gold nanoparticle sandwiches. Nano Lett 2008;8:485–90.

[4] Taminau TH, Stefani FD, Segerink FB, van Hulst NF. Optical antennas direct single-molecule emission. Nat Photon 2008;2:234–7.

[5] Taminau TH, Stefani FD, Van Hulst NF. Single emitters coupled to plasmonic nano-antennas: angular emission and collection efficiency. New J Phys 2008;10:1–16.

[6] Acuna GP, Bucher M, Stein IH, Steinhauer C, Kuzyk A, Holzmeister P, Schreiber R, Moroz A, Stefani FD, Liedl T, Simmel FC, Tinnefeld P. Distance dependence of single-fluorophore quenching by gold nanoparticles studied on DNA origami. ACS Nano 2012;6:3189–95.

[7] Anger P, Bharadwaj P, Novotny L. Enhancement and quenching of single-molecule fluorescence. Phys Rev Lett 2006;96:113002.1–113002.4.

[8] Kuhn S, Hakanson U, Rogobete L, Sandoghdar V. Enhancement of single-molecule fluorescence using a gold nanoparticle as an optical nanoantenna. Phys Rev Lett 2006;97:017402.1–017402.4.

[9] Bharadwaj P, Novotny L. Spectral dependence of single molecule fluorescence enhancement. Opt Express 2007;15:14266–74.

[10] Chhabra R, Sharma J, Wang H, Zou S, Lin S, Yan H, Lindsay S, Liu Y. Distance-dependent interactions between gold nanoparticles and fluorescent molecules with DNA as tunable spacers. Nanotechnology 2009;20:485201.1–485201.4.

[11] Busson MP, Rolly B, Stout B, Bonod N, Bidault S. Accelerated single photon emission from dye molecule-driven nanoantennas assembled on DNA. Nat Commun 2012;3:962.1–962.6.

[12] Busson MP, Rolly B, Stout B, Bonod N, Wenger J, Bidault S. Photonic engineering of hybrid metal-organic chromophores. Angew Chem Int Ed Engl 2012;51:11083–7.

[13] Hung AM, Micheel CM, Bozano LD, Osterbur LW, Wallraff GM, Cha JN. Large-area spatially ordered arrays of gold nanoparticles directed by lithographically confined DNA origami. Nat Nanotechnol 2010;5:121–6.

[14] Acuna GP, Moller FM, Holzmeister P, Beater S, Lalkens B, Tinnefeld P. Fluorescence enhancement at docking sites of DNA-directed self-assembled nanoantennas. Science 2012;338:506–10.

[15] Rothemund PW, Folding DNA to create nanoscale shapes and patterns. Nature 2006;440:297–302.

[16] Douglas SM, Marblestone AH, Teerapittayanon S, Vazquez A, Church GM, Shih WM. Rapid prototyping of 3D DNA-origami shapes with caDNAno. Nucleic Acids Res 2009;37:5001–6.

[17] Torring T, Voigt NV, Nangreave J, Yan H, Gothelf KV. DNA origami: a quantum leap for self-assembly of complex structures. Chem Soc Rev 2011;40:5636–46.

[18] Ding B, Deng Z, Yan H, Cabrini S, Zuckermann RN, Bokor J. Gold nanoparticle self-similar chain structure organized by DNA origami. J Am Chem Soc 2010;132:3248–9.

[19] Schmied JJ, Forthmann C, Pibiri E, Lalkens B, Nickels P, Liedl T, Tinnefeld P. DNA origami nanopillars as standards for three-dimensional superresolution microscopy. Nano Lett 2013;13:781–5.

[20] Douglas SM, Dietz H, Liedl T, Hogberg B, Graf F, Shih WM. Self-assembly of DNA into nanoscale three-dimensional shapes. Nature 2009;459:414–8.

[21] Stangl T, Bange S, Schmitz D, Wursch D, Hoger S, Vogelsang J, Lupton JM. Temporal switching of Homo-FRET pathways in single-chromophore dimer models of pi-conjugated polymers. J Am Chem Soc 2013;135:78–81.

[22] Ming T, Zhao L, Yang Z, Chen H, Sun L, Wang J, Yan C. Strong polarization dependence of plasmon-enhanced fluorescence on single gold nanorods. Nano Lett 2009;9:3896–3903.